

Jiří URBAN*

Brno University of Technology

THE PHYSICALLY NONLINEAR MODELLING OF THE STRESS-RIBBON FOOTBRIDGE SEGMENT

Summary. At present the Department of Concrete and Masonry Structures of the Brno University of Technology runs the research of the behaviour of the High Performance Concrete (HPC). The paper shows possibilities of today computational programmes in the physically nonlinear modelling of structural members. The paper focuses at the behaviour of a reinforced concrete segment of a stress-ribbon footbridge cast from HPC and his maximum load-bearing capacity. By means of the structural FE programme ATENA 2D is examined the nonlinear behaviour of the concrete after cracking and the post-peak behaviour of the segment. For comparison, there are presented outcomes from real-time laboratory testing of the above mentioned segment.

FIZYCZNE NIELINIOWE MODELOWANIE WZMOCNIENÍ ŻELBETOWYCH

Streszczenie. Instytut Konstrukcji Betonowych i Murowych Politechniki Brno prowadzi badania zachowania się betonu o dużej wytrzymałości (HPC). Artykuł pokazuje możliwości obliczeniowe żelbetowych kładek dla pieszych, a w szczególności skupia się na określeniu maksymalnego ich obciążenia. Dzięki programowi ATENA 2D możliwe jest przeanalizowanie zachowania się konstrukcji żelbetowej pracującej pozasprężyście. Dla porównania przedstawiono rezultaty badań laboratoryjnych.

1. The stress ribbon footbridge supported by an arch

The bridge crosses the freeway R3508 that is being built near city of Olomouc, Czech Republic. The bridge is formed by a stress-ribbon of two spans that is supported by an arch – see Fig. 1. The stress-ribbon of the length of 79.2 m is assembled of precast segments supported and post-tensioned by external tendons.

* Opiekun naukowy: Prof. Ing. Jiří STRÁSKÝ, CSc.

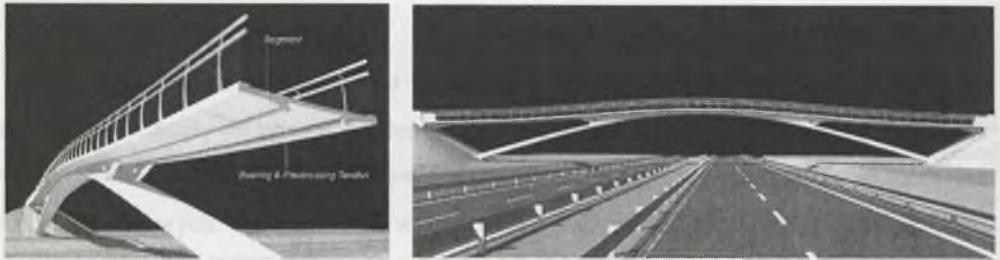


Fig. 1. Structural system and the longitudinal view
 Rys. 1. System strukturalny oraz widok

The geometry of the structure, the load and level of the post-tensioning are designed in such a way that horizontal force in the stress-ribbon and in the arch has the same magnitude.

Since the arch footings and stress-ribbon anchor blocks are connected together by compression struts, the bridge functions as a self anchored structure that load the footings by vertical reactions only.

The precast segments are designed of high-strength concrete of the compressive strength of 80 MPa, the cast-in-place arch of a high-strength concrete of strength 70 MPa. The external cables are anchored at the end abutments and deviated on saddles formed by the arch crown and short spandrel walls. At the abutments the tendons are supported by short saddles formed by cantilevers protruded from the anchor blocks. The stress-ribbon and the arch are rigidly connected at the central of the bridge. The arch footings are founded on drill shafts, the anchor blocks on micro-piles.

2. Finite element model of the precast segment in ATENA 2D

2.1. Geometry of the studied segment

The shape of the segment is shown in Fig. 2. Since the segment was cast from high-strength concrete C70/80, the reinforcement was designed unconventionally in the form of just one steel grid in the middle of the height of the segment ($\varnothing 8$, net 100/100 mm) – Fig. 3.

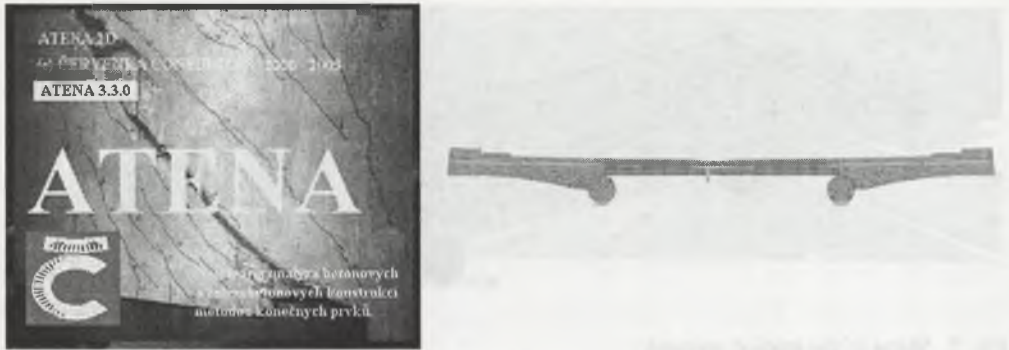


Fig. 4. The welcome window of the ATENA 2D and the FE model of the segment
Rys. 4. Okno ATENA 2D i model FE

In CAD-like pre-processing of ATENA was created 2D plane-stress structural model – see Fig. 4, with following material models for particular parts of the segment: for concrete was used non-linear material model SBETA with ultimate strength $R_{cu} = 70$ MPa (other material characteristics such as tension and compressive strengths, fracture energy etc. are automatically generated according to CEB, fib, RILEM formulas); for reinforcing steel was chosen bi-linear material model with hardening - $f_{yk} = 490$ MPa, $f_{tk} = 540$ MPa, with full bond; for steel plates spreading the load into concrete parts was chosen plane-stress elastic material with $E = 210$ MPa; and finally for interface between concrete and steel parts was chosen 2D-contact material with compressive stiffness of $2e8$ MN/m³ and with zero tension strength i.e. $R_t = 0$ MPa.

Non-linear solution in ATENA proceeds in load steps, where in each load step the iteration of *Newton-Raphson method* is performed until the equilibrium is achieved. Programme is also capable to solve a post-peak behaviour of the structure at the descending side of the load-deflection diagram, which is achieved by employing numerical solution of Arc-length method. The solution is formulated in the field of large-displacements theory, thus incorporate geometrically-nonlinear behaviour as well. The great advantage of the programme is graphical representation of the behaviour of the structure during the solution, which shows interactive load-deflection diagram, deformation states and propagation of cracks in real time of solving.

2.3. Performed analysis

The segment was subjected to maximum attainable sagging and hogging moment in order to inspect worst case of loading of the structure – see Fig. 5. Subsequently, the segment was tested for the four cases of possible loading by a small truck or ambulance car, which is the maximum possible true load that could appear on the bridge during his lifetime – Fig. 6.



Fig. 5. Load producing maximum sagging and hogging moment

Rys. 5. Maksymalne obciążenia

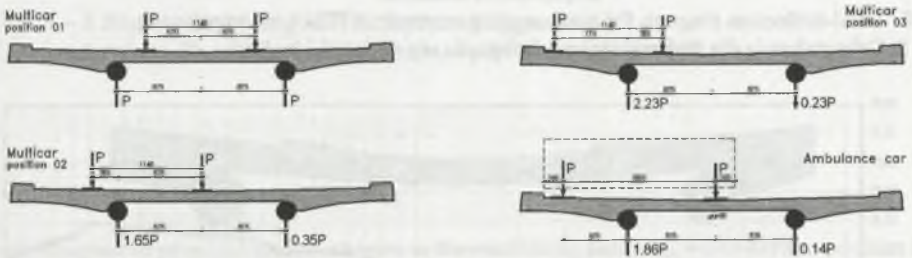


Fig. 6. Cases of possible loading by a small truck or ambulance car

Rys. 6. Przypadki możliwego ładowania przez małą ciężarówkę lub ambulans

2.4. Test results

For cases of maximum sagging and hogging moments are plotted diagrams of principal compressive ($s_{min,c}$) and tension stresses ($s_{max,c}$) in the concrete and principal tension stresses ($s_{max,s}$) in the reinforcing steel at the ultimate limit state – see Fig.7. These two cases were also tested at the laboratory and hence it was possible to confront the outcomes with ATENA.



Fig. 7. $s_{min,c}$, $s_{max,c}$ and $s_{max,s}$ for max. sagging (left) and max. hogging moment (right)

Rys. 7. $s_{min,c}$, $s_{max,c}$ i $s_{max,s}$ dla maksymalnych obciążeń

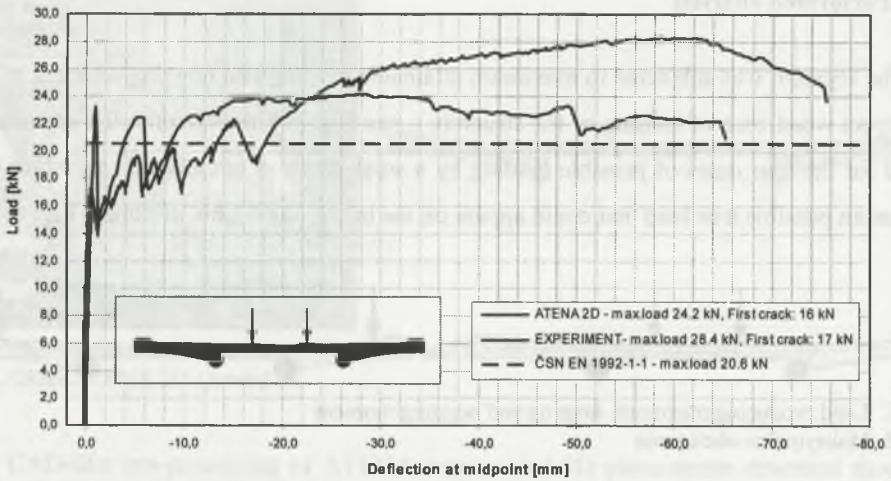


Fig. 8. Load-deflection diagram for max. sagging moment: ATENA vs. experiment

Rys. 8. Odształcenia dla maksymalnego obciążenia wg obliczeń i badań

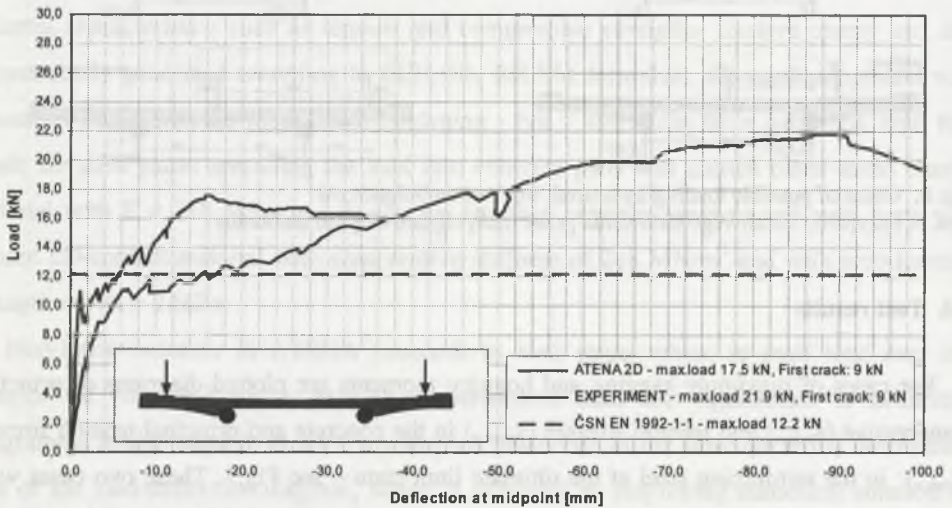


Fig. 9. Load-deflection diagram for max. hogging moment: ATENA vs. experiment

Rys. 9. Odształcenia dla obciążenia ekstremalnego wg obliczeń i badań

The Figs. 8 and 9 show the match of the experimentally gained data with data obtained by FE modelling of the segment in ATENA 2D.

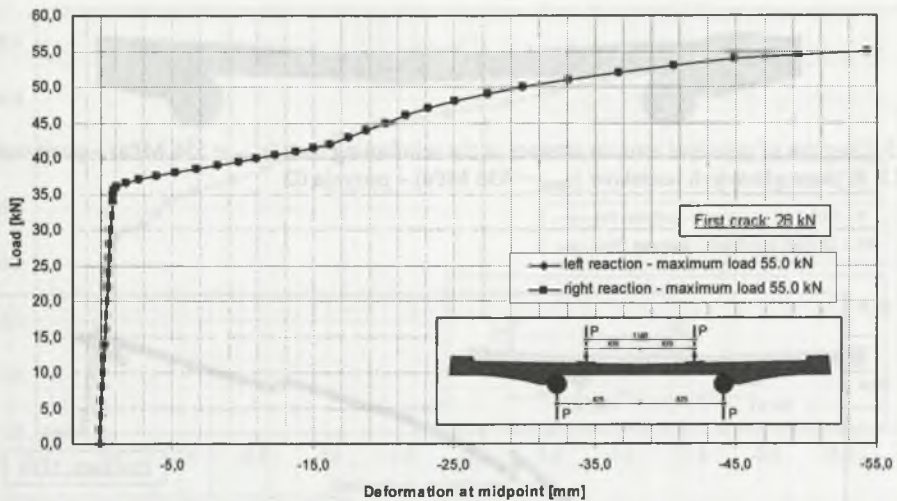


Fig. 10. L - d diagram for loading with the light truck in position 01

Rys. 10. L - d wykres dla załadowywania z lekką ciężarówką na miejscu 01



Fig. 11. Diagram of principal tension stresses in the reinforcing bars ($s_{max} = 513$ MPa) – position 01

Rys. 11. Wykres głównych nacisków ($s_{max} = 513$ MPa) – pozycja 01

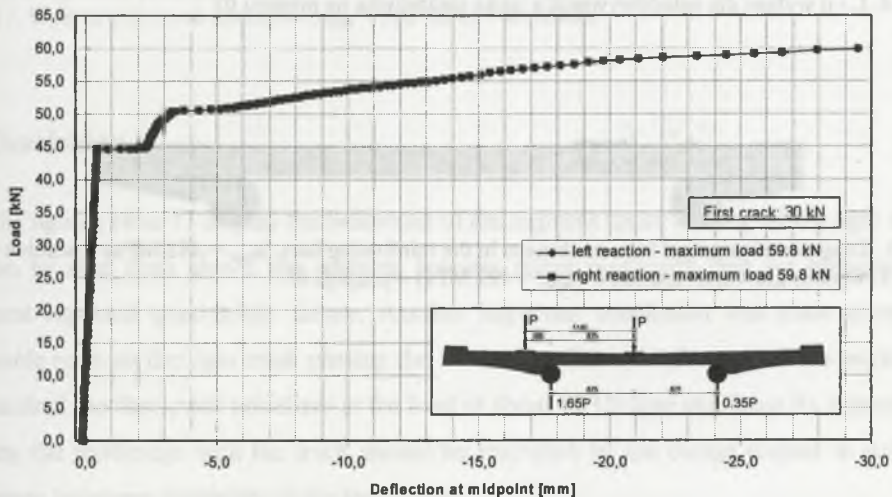


Fig. 12. L - d diagram for loading with the light truck in position 02

Rys. 12. L - d wykres dla załadowywania z lekką ciężarówką na miejscu 02



Fig. 13. Diagram of principal tension stresses in the reinforcing bars ($s_{\max} = 536 \text{ MPa}$) – position 02
 Rys. 13. Wykres głównych nacisków ($s_{\max} = 536 \text{ MPa}$) – pozycja 02

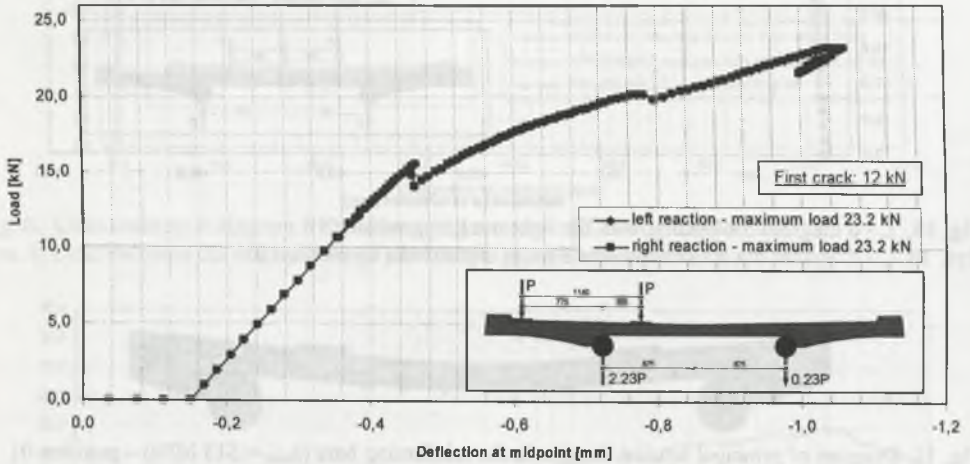


Fig. 14. L - d diagram for loading with the light truck in position 03
 Rys. 14. L - d wykres dla załadowywania z lekką ciężarówką na miejscu 03

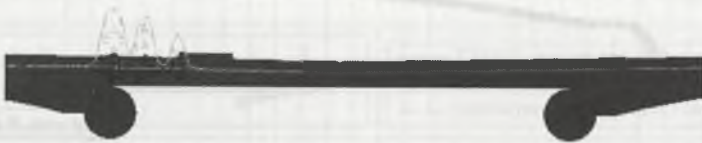


Fig. 15. Diagram of principal tension stresses in the reinforcing bars ($s_{\max} = 492 \text{ MPa}$) – position 03
 Rys. 15. Wykres głównych nacisków ($s_{\max} = 492 \text{ MPa}$) – pozycja 03

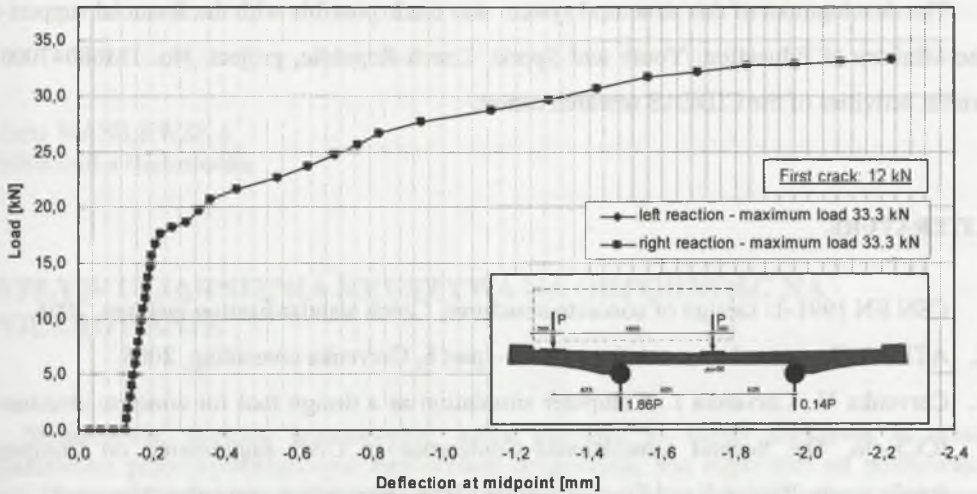


Fig. 16. L - d diagram for loading with the ambulance car

Rys. 16. L - d wykres dla obciążeń ambulansem



Fig. 17. Diagram of principal tension stresses in the reinforcing bars ($s_{\max} = 522$ MPa) – ambulance car

Rys. 17. Wykres głównych nacisków ($s_{\max} = 522$ MPa) – ambulans

3. Conclusion

The figures 10 to 17 display the behaviour of the segment under loading with a light truck. As can be seen from above, the segment behaves rather plastically than for high-strength concrete expected quasi-brittle failure. Another important conclusion was made about the allowable route of the light truck passing the footbridge. Since for the path of the truck near the handrail the first crack initializes at the load of about 12 kN (per one force P), this path of passing the footbridge with the truck should be restricted by the design project in order to guarantee long-term durability of the footbridge.

Regarding the ultimate limit state, the ultimate load-bearing capacity of all possible loading cases was achieved by yielding of reinforcement bars at the location with maximum opened crack, what assures high ductility of the precast segment.

The development of this structural system was made possible with the financial support of the Ministry of Education, Youth and Sports, Czech Republic, project. No. 1M680470001, within activities of the CIDEAS research center.

LITERATURE

1. ČSN EN 1991-1: Design of concrete structures, Czech standardization institute, 2006.
2. ATENA: Program documentation, part 1 – part 6, Cervenka consulting, 2006.
3. Cervenka V., Cervenka J.: Computer simulation as a design tool for concrete structures, ICCE-96, The Second International Conference in Civil Engineering on Computer Applications, Research and Practise Bahrain 1996 (<http://www.cervenka.cz/papers>).

Recenzent: Prof. dr hab. inż. Wojciech Radomski